



Analysis of unsymmetrical faults based on artificial neural network using 11 kV distribution network of University of Lagos as case study

Akintunde S. Alayande ^a, Ignatius K. Okakwu^b, Olakunle E. Olabode ^{c,*},
Okwuchukwu K. Nwankwoh ^d

^{a, d} Department of Electrical and Electronics Engineering, University of Lagos, Lagos, Nigeria

^b Department of Electrical and Electronics Engineering, Olabisi Onabanjo University, Ago-Iwoye, Nigeria

^c Department of Electrical, Electronics and Computer Engineering, Bells University of Technology, Ota, Nigeria

ARTICLE INFO

Article history:

Received 27 June 2020

Received in revised form
3 August 2020

Accepted 11 September 2020

Available online
24 September 2020

Keywords:

Artificial neural network

Back-propagation

Fault analysis

Fault classification

Fault detection

ABSTRACT

The occurrence of faults in any operational power system network is inevitable, and many of the causative factors such as lightning, thunderstorm among others is usually beyond human control. Consequently, there is the need to set up models capable of prompt identification and classification of these faults for immediate action. This paper, explored the use of artificial neural network (ANN) technique to identify and classify various faults on the 11 kV distribution network of University of Lagos. The ANN is applied because it offers high speed, higher efficiency and requires less human intervention. Datasets of the case study obtained were sectioned proportionately for training, testing, and validation. The mathematical formulations for the method are presented with python used as the programming tools for the analysis. The results obtained from this study, for both the voltage and current under different scenarios of faults, are displayed in graphical forms and discussed. The results showed the effectiveness of the ANN in fault identification and classification in a distribution network as the model yielded satisfactory results for the available limited datasets used. The information obtained from this study could be helpful to the system operators in faults identification and classification for making informed decisions regarding power system design and reliability.

1. Introduction

Modern electrical power systems can be regarded as a pivot supporting virtually all activities of man required to enhance meaningful existence. Smart home and industrial automation are examples of areas of applications where the benefits of an electrical energy is greatly appreciated in almost every

part of the world [1]. Hence, stern efforts to sustain the optimum operation of power systems at all times become non-negotiable.

Over time, experiences had shown that fault is one of the major anomalies in power systems, capable of causing a major setback to optimum performance and operation of power systems [2]. When the fault occurred,

* Corresponding author

E-mail address: oeolabode@bellsuniversity.edu.ng

<https://doi.org/10.37121/jase.v4i1.91>

current and voltage magnitudes suffer severe deviations from their normal magnitudes. Consequently, it triggers protective devices to act, which when it is severe than what proactive devices can cope with, such dangerous magnitudes are passed on to delicate power systems equipment like generators, transformers, insulator and many others [3]. Hence, damage to these sensitive pieces of equipment cannot an option. As a matter of fact, the emergence of faults would have been of no significance, if the system is intelligent enough to detect and forestall possible faults even before they arise.

Simulation software is an essential tool in recent time, which permits analysis of large interconnected systems in real-time [4], [5]. For instance, the authors in [6], [7] utilized the classical PSPICE to observe power system operations especially with the presence of a switching feature. PSPICE is capable of modeling the essential circuit equations at both transient and steady states. It can as well be used to set up a database for managing load flow data, field test results and various other engineering information as seen in [8], [9]. However, the PSPICE simulation platform is limited to low frequency-dependent devices [10]. Similarly, system's distance calculation technique based on the fault distance estimation re-action method, using data from one transmission line terminal was used by the authors of [11].

In recent time, there are several artificial intelligence approaches to detect and classify fault on the power system. Such approaches include wavelet transform [12], a fuzzy logic technique [13], short Fourier transform [14], continuous wavelet transform, adaptive neuro-fuzzy inference system (ANFIS) [15], and artificial neural network [16]. ANN was found to enjoy wide usage when it comes to fault detection and classification. For instance, the authors of [17] classified and detected location of faults within a power transmission network using ANN. Similarly, the authors in [18] advanced the work done reported in [17] by implementing identification, classification and detection of fault location using ANN. Also, an analysis of the different types of faults on the Nigerian 33-kV transmission network using ANN was carried out by the authors of [19]. More recently, various methodologies for fault classifications and detection based on ANN are reviewed in [20].

Every power system strives for its sustainability. Consequently, in some

developing countries like Nigeria, where the demand for electricity outweighs the power produced, it is economical to ensure that the available generated power is optimally distributed. As the occurrence of faults in power system operation is inevitable, its emergence could be catastrophic, which could lead to total blackout or voltage collapse of the system. In order to promptly salvage the situation and ensure power system sustainability, it is necessary to analyze and classify faults in real-time. This can help power system engineers in quickly identifying the type of fault that has ensued so as to take quick decision to maintain the integrity of the network. Every occurrence of fault is characterized by variance in current and voltage values. These faults are associated with patterns of currents and voltage distributions. The neural network features a connection of neurons that takes in datasets for each type of fault, which learns and recognizes the patterns for voltage and current distribution for each type of fault. As such, it is able to accurately analyze and predict the type of fault whenever it re-emerges in the system.

Although several works have been reported on fault classification, detection and location on transmission networks [21]–[24], less attention has been paid to fault classification, identification and location detection on the 11-kV practical distribution network. This paper presents the application of an ANN for symmetrical fault analysis on a typical 11-kV distribution network in Nigeria.

The remaining section of this paper takes the following structure: section 2 presents the theoretical framework as well as the mathematical formulations of the method with reference to the artificial neural networks and the analysis of an unsymmetrical fault in a distribution network. The results are presented and discussed in section 3 while the paper is concluded in section 4.

2. Theoretical Framework and Mathematical Modeling

2.1. ANN-Based Fault Analysis

Artificial neural networks (ANN) or connectionist systems are computing systems based on biological neural networks that make up animal brains [25]. Neural network has been viewed as framework rather than been called an algorithm, which enhances several differ machine learning algorithms not only to

work together but also process complex inputs data [26], [27].

Such systems are capable of learning pattern based on some set of rules used in training dataset with a view to execute dedicated tasks [28]. ANN works on fundamental principles of central and peripheral nervous systems such that it observes, learns and processes patterns from datasets with sole aim to make decisions on an entirely new set of data [29], [30]. It essentially comprised the input, the hidden layer that processes the input, the output and the neurons that carry the information. Artificial neurons are assembled into layers. It has a weight that is adjusted as learning progresses; the weight of a connection increases or decreases the strength of the signal [30]. Artificial neurons may have a threshold to send the signal only if that threshold is crossed by the aggregate signal. Different layers may perform different kinds of transformations on their inputs, such that signals from the first layer to the last layer are traversing the layers in a quite number of times.

Consider the skeletal structure of Fig. 1 based on back propagation of the ANN as shown in Fig. 2.

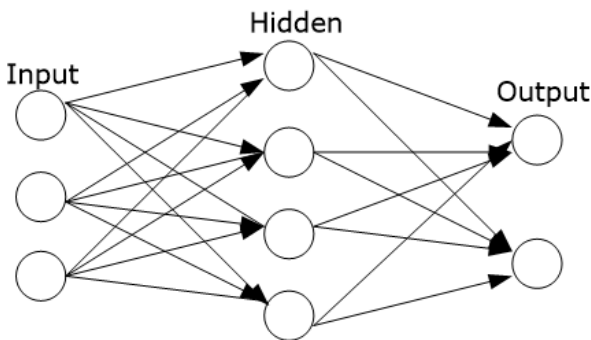


Fig. 1 Basic structure of an ANN.

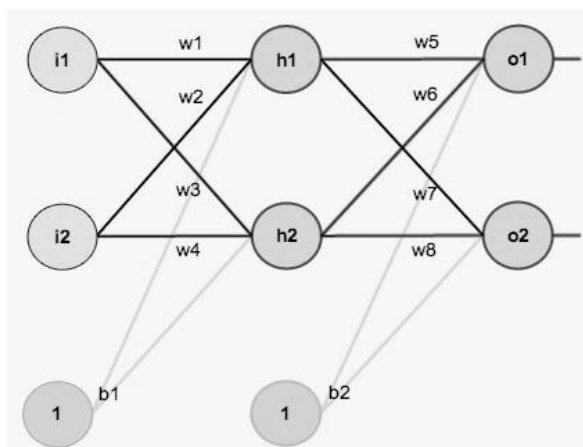


Fig. 2 The neural network's skeletal structure [31].

Given that $i1, i2$ are primary inputs, $h1, h2$ are neurons (hidden layer), $o1, o2$ are output neurons, $b1, b2$ are biases and $w1, \dots, w8$ are the weights. As shown in Fig. 2, the net input (net_{h1}) and output (out_{h1}) at $h1$ can be expressed respectively as:

$$net_{h1} = w1 * i1 + w2 * i2 + b * 1. \tag{1}$$

$$out_{h1} = \frac{1}{1+e^{-net_{h1}}}. \tag{2}$$

Similarly, the output from $h2$ can be written as:

$$out_{h2} = \frac{1}{1+e^{-net_{h2}}}. \tag{3}$$

The net input (net_{o1}) and output (out_{o1}) to node $o1$ respectively are:

$$net_{o1} = w5 * out_{h1} + w6 * out_{h2} + b * 1. \tag{4}$$

$$out_{o1} = \frac{1}{1+e^{-net_{o1}}}. \tag{5}$$

In a similar manner, the output from $o2$ is given by the equation:

$$out_{o2} = \frac{1}{1+e^{-net_{o2}}}. \tag{6}$$

The total error is given as:

$$E_{total} = \sum \frac{1}{2} (target - output)^2. \tag{7}$$

$$E_{total} = E_{o1} + E_{o2}. \tag{8}$$

In a bid to describe how the errors are influenced by the weights at each synaptic junction, the rate of change of the error was evaluated with respect to each weight. Considering $w5$ for example, to evaluate how the error is affected by $w5$, a partial derivative of the error was determined with respect to the weight $w5$ using chain's rule as:

$$\frac{\partial E_{total}}{\partial w5} = \frac{\partial E_{total}}{\partial out_{o1}} * \frac{\partial out_{o1}}{\partial net_{o1}} * \frac{\partial net_{o1}}{\partial w5}. \tag{9}$$

$$E_{total} = \frac{1}{2} (target_{o1} - out_{o1}) + \frac{1}{2} (target_{o2} - out_{o2}) \tag{10}$$

$$\begin{aligned} \frac{\partial E_{total}}{\partial out_{o1}} &= 2 * \frac{1}{2} (target_{o1} - out_{o1}) * (-1) + 0 \\ &= -(target_{o1} - out_{o1}). \end{aligned} \tag{11}$$

Thus,

$$out_{o1} = \frac{1}{1+e^{-net_{o1}}}, \tag{12}$$

$$\frac{\partial out_{o1}}{\partial net_{o1}} = out_{o1} (1 - out_{o1}), \tag{13}$$

and

$$net_{o1} = w5 * out_{h1} + w6 * out_{h2} + b * 1. \tag{14}$$

$$\frac{\partial net_{o1}}{\partial w5} = 1 * out_{h1} * w5^{(1-1)} + 0 + 0 = out_{h1}. \tag{15}$$

Therefore,

$$\frac{\partial E_{total}}{\partial w5} = \frac{\partial E_{total}}{\partial out_{o1}} * \frac{\partial out_{o1}}{\partial net_{o1}} * \frac{\partial net_{o1}}{\partial w5}$$

$$= -(target_{o1} - out_{o1}) * out_{o1}(1 - out_{o1}) * out_{h1}. \quad (16)$$

Alternatively,

$$\frac{\partial E_{total}}{\partial w5} = \delta_{o1} * out_{h1}. \quad (17)$$

Where,

$$\delta_{o1} = \frac{\partial E_{total}}{\partial out_{o1}} * \frac{\partial out_{o1}}{\partial net_{o1}}. \quad (18)$$

To reduce the error, a learning rate (for the model) was introduced and the result was subtracted from the initial weight ($w5$ in this case). The new weight can be written as:

$$w5^+ = w5 - \eta * \frac{\partial E_{total}}{\partial w5}. \quad (19)$$

The process is carried out for each weight and iterated until a desired output is obtained.

2.2. Unsymmetrical Faults Analysis

In the balanced three-phase fault, all three phases are either mutually shorted by one another or are equally shorted to the ground. This implies that all three phases experience the same degree of fault with a 120° phase displacement. This means that calculations can be done using a single phase (since whatever happens in one of the three phases translates to the rest). During fault simulations, impedance is attached to the associated fault area and the resulting faulty network is evaluated using Thevenin's equivalent circuit as observed from the fault location. Prior to the occurrence, the system is assumed to be stable and a single phase is taken for analysis; where the generator is taken as a constant voltage source with its associated impedance. Consider a conventional n -bus system shown in Fig. 3(a) with a fault occurring at bus R of the system. The system can be re-modeled as shown in Fig. 3(b), setting all voltage sources to zero and replacing them by their corresponding impedance values. To evaluate the fault, a voltage $V_f(0)$ is applied to the faulted bus and a fault impedance Z_f is attached to the bus so that the fault current I_f will flow through Z_f . If the vector of the system pre-fault voltage is given by [32] as:

$$[V_{BUS}] = [V_1(0) V_2(0) \dots V_r(0)]^T. \quad (20)$$

In the event of a fault, there is a change in the bus voltages given by the matrix $[\Delta V_{BUS}]$ due to the current I_f flowing through Z_f .

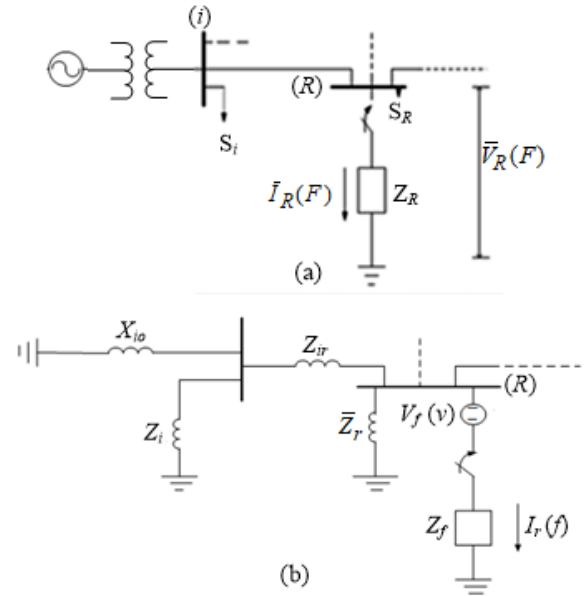


Fig. 3 One-line diagrams (a) faulty n -bus system with the fault at the R^{th} bus [32] (b) the re-modeled network.

If Z_i represents equivalent impedance at bus (i), Z_r represents equivalent impedance at bus (r) (faulted bus), Z_{ir} connotes line impedance between buses (i) and (r), X_{io} stands for equivalent reactance of generator at bus (i), Z_f represents the fault impedance introduced at (r), $I_r(f)$ represents the fault current at (r) flowing through Z_f , and $V_f(v)$ denotes the voltage applied at faulted bus (r). The voltage at fault condition can be expressed as [32]:

$$V_{BUS}(f) = V_{BUS}(0) - \Delta V_{BUS}. \quad (21)$$

Where, $V_{BUS}(f)$ is the matrix for the voltage at the different buses during fault, $V_{BUS}(0)$ is the matrix for the pre-fault voltage values prior to fault and ΔV_{BUS} is the matrix for the drop in voltage values at the different buses during fault.

The vector of the bus currents for the network can be expressed as follows:

$$I_{BUS} = V_{BUS} Y_{BUS}. \quad (22)$$

Where, V_{BUS} is the vector of bus voltage profile and Y_{BUS} is the $n - by - n$ bus admittance matrix for the network.

In the event of fault, all voltage sources at the different buses (except the bus on which the fault occurs) are shorted and represented by their equivalent resistances. The implication of this is that current in every other bus aside the faulted bus is 0 as the faulted bus has a voltage $V_r(0)$ applied to it. Therefore, equation (22) can be expanded as [32]:

$$\begin{bmatrix} 0 \\ \vdots \\ I_r(F) \\ \vdots \\ 0 \end{bmatrix} = \begin{bmatrix} Y_{11} \wedge Y_{1r} \wedge Y_{1n} \\ M \\ Y_{r1} \wedge Y_{rr} \wedge Y_{rn} \\ M \\ Y_{n1} \wedge Y_{nr} \wedge Y_{nn} \end{bmatrix} \begin{bmatrix} \Delta V_1 \\ \vdots \\ \Delta V_r \\ \vdots \\ \Delta V_n \end{bmatrix} \tag{23}$$

From equation (22), the vector of change in the bus voltage magnitude is given by the equation:

$$[\Delta V_{BUS}] = [Y_{BUS}]^{-1}[I_{BUS}] \tag{24}$$

But,

$$[V_{BUS}(f)] = [V_{BUS}(0)] - [\Delta V_{BUS}] \tag{25}$$

$$[V_{BUS}(f)] = [V_{BUS}(0)] - [V_{BUS}(0)][I_{BUS}] \tag{26}$$

In compact form,

$$\begin{bmatrix} V_1(F) \\ \vdots \\ V_r(F) \\ \vdots \\ V_n(F) \end{bmatrix} = \begin{bmatrix} V_1(0) \\ \vdots \\ V_r(0) \\ \vdots \\ V_n(0) \end{bmatrix} - \begin{bmatrix} Z_{11} & \dots & Z_{1r} & \dots & Z_{1n} \\ \vdots & & \vdots & & \vdots \\ Z_{r1} & \dots & Z_{rr} & \dots & Z_{rn} \\ \vdots & & \vdots & & \vdots \\ Z_{n1} & \dots & Z_{nr} & \dots & Z_{nn} \end{bmatrix} \begin{bmatrix} (0) \\ \vdots \\ I_r(F) \\ \vdots \\ 0 \end{bmatrix} \tag{27}$$

In a situation whereby the effect of the fault is not evenly distributed across all three phases, the use of symmetrical components employed in evaluating the current and voltage values during a fault is given as [32]:

$$a = a_1 + a_2 + a_0 \tag{28a}$$

$$b = b_1 + b_2 + b_0 \tag{28b}$$

$$c = c_1 + c_2 + c_0 \tag{28c}$$

Similarly, each phase in terms of phase A can be represented as follows:

$$a = a_0 + a_1 + A_2; \tag{29a}$$

$$b = a_0 + K^2 a_1 + K a_2; \tag{29b}$$

$$c = a_0 + K a_1 + K^2 a_2; \tag{29c}$$

where, K is an operator defined by $K = 1 \angle 120^\circ$.

Equation (29) can be written in matrix form as follows:

$$\begin{bmatrix} a \\ b \\ c \end{bmatrix} = \begin{bmatrix} 1 & 1 & 1 \\ 1 & K^2 & K \\ 1 & K & K^2 \end{bmatrix} \begin{bmatrix} a_0 \\ a_1 \\ a_2 \end{bmatrix} \tag{30}$$

$$\text{If } X = \begin{bmatrix} 1 & 1 & 1 \\ 1 & K^2 & K \\ 1 & K & K^2 \end{bmatrix}; \tag{31}$$

the inverse of X can be estimated by using the relation:

$$X^{-1} = \frac{1}{3} \begin{bmatrix} 1 & 1 & 1 \\ 1 & K^2 & K \\ 1 & K & K^2 \end{bmatrix} \tag{32}$$

The phase currents and sequence currents, using symmetrical components, can be written as:

$$[I]_{abc}^T = X[I]_{012}^T \tag{33}$$

$$[I]_{012}^T = X^{-1}[I]_{abc}^T \tag{34}$$

In a similar fashion, the phase and sequence voltages, can be written respectively as:

$$[V]_{abc}^T = X[V]_{012}^T \tag{35}$$

$$[V]_{012}^T = X^{-1}[V]_{abc}^T \tag{36}$$

The proposed method is then extended to the 11 kV distribution network of the University of Lagos to test the effectiveness of its performance. Different simulations and signal analysis are performed in the MATLAB Integrated Development Environment (IDE).

2.3. Implementation

The University of Lagos 11 kV distribution station comprises eleven buses, two incoming and nine out-going, with a power outputs such that $3.5 \text{ MW} \leq P_{output} \leq 5.5 \text{ MW}$ is used to implement the approach presented in this study. This section discusses, in detail, the implementation and testing of the neural network model.

2.3.1. Model training: The datasets were obtained from the station and used to train, test and evaluate the performance of the model. Table 1 shows the data set employed for the training model. The datasets were normalized against the preset values before being fed into the neural network model.

A multi-layer perceptron (MLP) was deployed in creating a model for the neural-network, it combines a feed-forward and a supervised learning technique called a back-propagation. The feed forward simply combines all available sets of neurons and the back propagation compares the outputs obtained, calculates the error, differentiates the error function to obtain the global minimum and then adjusts the neurons weights and biases until the desired output is obtained to a reasonable accuracy. The accuracy obtained for training the model was found to be 90 %. However, this was due to the relatively little data that was available for testing the model. The sci-kit learn library was adopted in building this library and obtaining necessary statistical insights as to the model's performance. The data in Table 1 was properly visualized and cleaned up so as to obtain unadulterated training results and a training plot was obtained.

2.3.2. Model testing: The next step after sufficient training is testing the model to observe performance and how it handles a new set of data. Table 2 shows the datasets

that were passed into the model via an excel spreadsheet. These datasets were used to assess the trained model to see how it fared and also to observe accuracy, error(s) and

regression. The test accuracy was found to be 100 % for the dataset that was tested and a validation plot as well as a confusion matrix was obtained for the test set.

Table 1 Training datasets.

V_a	V_b	V_c	I_a	I_b	I_c
0.5000	0.5000	0.5000	0.1500	0.1500	0.1500
0.0000	0.4800	0.4800	0.8890	0.1570	0.1560
0.4800	0.0000	0.4300	0.1640	0.9270	0.1660
0.4800	0.4700	0.0000	0.0950	0.9330	0.8150
0.1160	0.1030	0.4300	0.7720	0.7722	0.1550
0.5000	0.1123	0.1078	0.1486	0.8880	0.8890
0.0000	0.4890	0.0750	0.7500	0.1570	0.7570
0.0150	0.0150	0.5100	0.8440	0.8440	0.1490
0.4870	0.0290	0.0289	0.1520	0.6667	0.7110
0.0920	0.5160	0.920	0.7740	0.1499	0.7660
0.1200	0.1250	0.1290	0.8200	0.7900	0.8900
1.0030	1.0211	1.0110	1.1120	1.1100	1.0992
0.0000	0.9480	0.9480	3.8890	1.1170	1.1065
1.0030	0.0000	1.0130	1.1640	3.9270	1.1660
1.1080	1.1072	0.0000	0.9500	0.9330	3.8150
0.4160	0.5300	1.0430	3.7720	3.6722	1.1150
1.1500	0.1230	0.2078	1.1486	4.8880	4.8810
0.0080	1.0890	0.2075	5.7500	0.9870	5.7510
0.0150	0.0150	1.1100	3.8440	4.0440	1.1020
1.0870	0.0290	0.0289	1.0520	3.6667	4.0110
0.0920	1.1160	0.0920	4.7740	1.1090	3.9660
0.3120	0.1050	0.1790	4.8200	4.8910	4.8900
1.0030	1.0040	0.9970	0.9930	0.9980	1.0010
0.2250	1.1120	1.1050	4.331	0.9860	0.9970
1.1150	0.3340	1.1030	0.9910	5.2210	1.0020
0.5530	0.3360	0.9860	4.4480	4.4480	1.0060
0.9920	0.5520	0.3380	0.9860	4.5560	4.5560
0.5510	1.0010	0.6630	6.2220	0.9940	6.2220
0.3240	0.3240	1.1160	6.1220	6.8870	0.9890
1.1130	0.3150	0.3150	0.9870	5.6670	6.1230
0.3020	1.1180	0.3020	7.2230	0.9960	6.8960

Note: V_a , V_b and V_c represent the normalized phase voltage values for phases a, b and c respectively; I_a , I_b and I_c represent the normalized phase current values for phases a, b and c respectively.

Table 2 Test datasets.

V_a	V_b	V_c	I_a	I_b	I_c
0.995	0.991	0.993	0.997	0.994	0.992
0.321	1.184	1.179	3.521	0.989	0.983
1.173	0.334	1.194	0.982	3.336	0.985
1.192	1.172	0.336	0.981	0.979	3.337
0.471	0.625	0.987	5.421	5.421	0.984
0.986	0.651	0.985	5.421	5.421	5.379
0.469	0.987	0.648	5.376	0.984	5.376
0.206	0.205	1.186	7.187	7.855	0.985
1.188	0.213	0.213	0.985	7.185	7.855
0.205	1.179	0.205	7.187	0.985	7.855

3. Results and Discussion

Fig. 4 shows the training curve for the model and the training accuracy obtained was found to be 90 %.

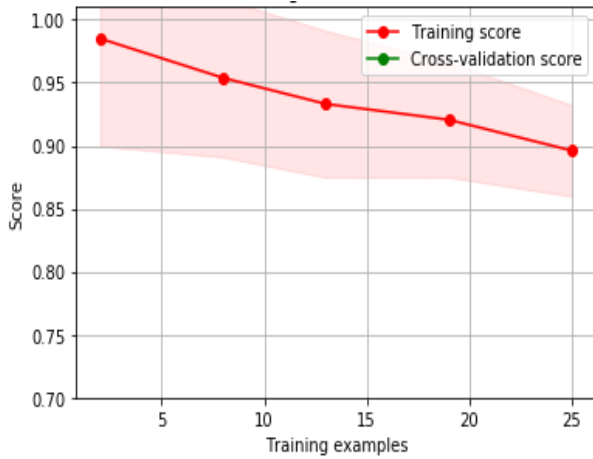


Fig. 4 ANN training curve with MLP.

3.1. Univariate Analysis of System Parameters

The univariate analysis of the voltage on each phase clearly buttresses the distinct corresponding trend in behavior of the voltage distribution across the pre-fault and on-fault conditions. Taking phase 'a', for instance, the voltage behavior is shown (Fig. 5). The blue shade behind the waveform is called a density plot and it describes the regions where the voltage values are represented for pre-fault and on-fault scenarios. The waveform represents voltage distribution across pre-fault and on-fault cases. On the left part of the waveform, the voltage value is closer to unity as with the normalized pre-fault values and then on the right side of the plot. It can be seen that a decline in voltage magnitude is experienced and this is essentially obtainable during fault conditions.

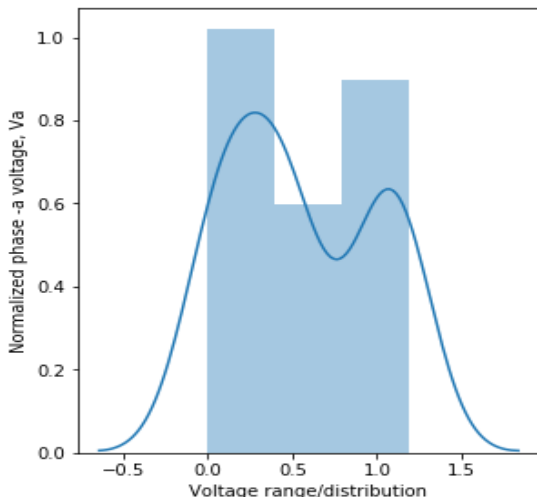


Fig. 5 Univariate plot showing voltage distribution for phases 'a'.

The normalized voltage axis as shown in Figs. 5 to 7 represents the normalized fault voltage values (phases a to c) and the voltage distribution axis shown in each of the figures represents the voltage value range for standard conditions. Each phase shows the voltage distribution for different points of operation and it can be seen that a voltage collapse occurs during a fault condition. Similar to phase 'a', phase 'b' shows the voltage distributions across different conditions. Also, phase 'a' and phase 'b' show the voltage distribution for different points of operation and it can be seen that a voltage collapse occurs during a fault condition.

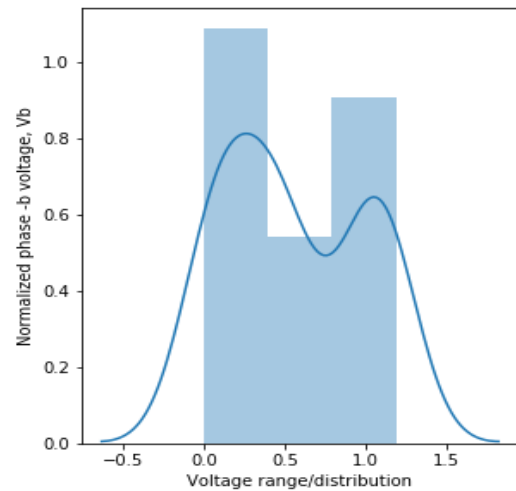


Fig. 6 Univariate plots for phase 'b' voltage distribution.

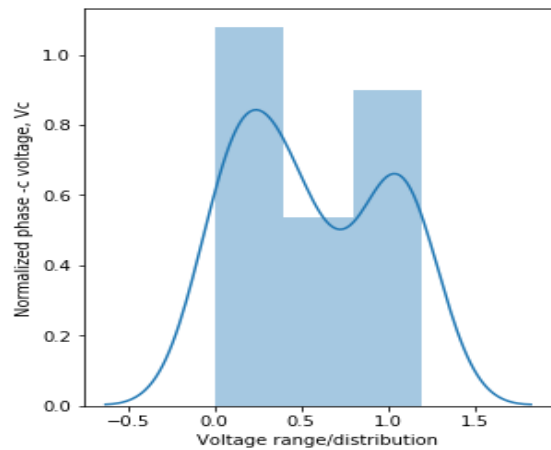


Fig. 7 Univariate plots for phase 'c' voltage distribution.

The univariate current distribution (Fig. 7) shows the trend in behavioral of current values during fault conditions (to the left of the curve) and during normal or pre-fault conditions. The univariate current distributions, shown in Figs. 8 to 10, show the trend in behavior of current values during fault conditions (to the left of the curve) and during normal or pre-fault conditions.

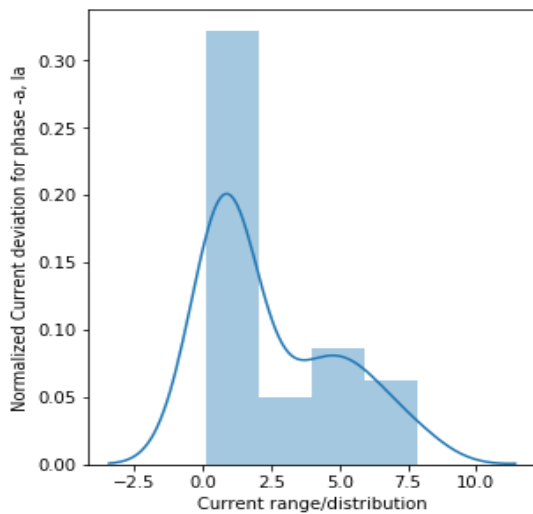


Fig. 8 Univariate plot showing current distribution for phase 'a'.

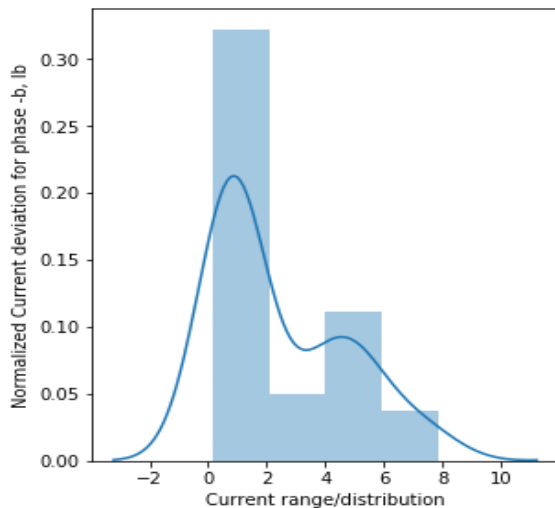


Fig. 9 Univariate plot showing current distribution for phase 'b'.

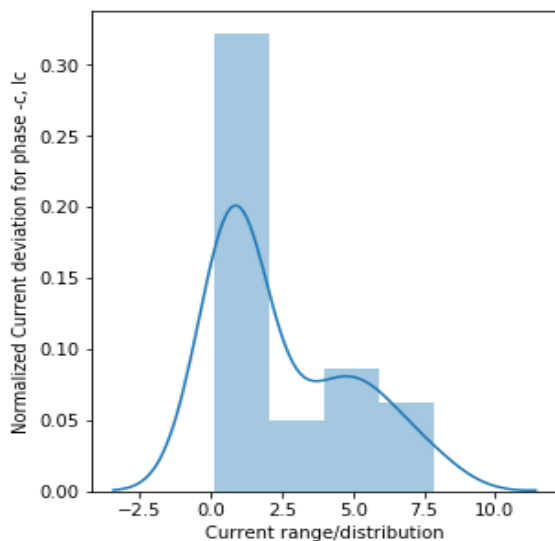


Fig. 10 Univariate plot showing current distribution for phase 'c'.

The normalized current deviation axis shows step sizes for the mean deviation of the current values while the Current distribution axis represents current distribution across pre-fault and on-fault conditions. Fig. 8 shows the distribution of the current data points and also shows a density plot for where the values are concentrated during pre-fault and on-fault scenarios for phase 'a'. The same applies to phase 'b' (Fig. 9). As with phases 'a' and 'b', Fig. 10 shows the univariate plot for the current distribution in phase 'c'.

3.2. Bivariate Analysis of System Parameters

The bivariate plot in Fig. 11 shows a stacked histogram plot of current and voltage values during fault conditions. On the left of the plot, the pre-fault voltage and current values can be seen on yellow and blue bars respectively (on a scale of 0.5 on the vertical axis) and on the right, the voltage collapse for both parameters is observed.

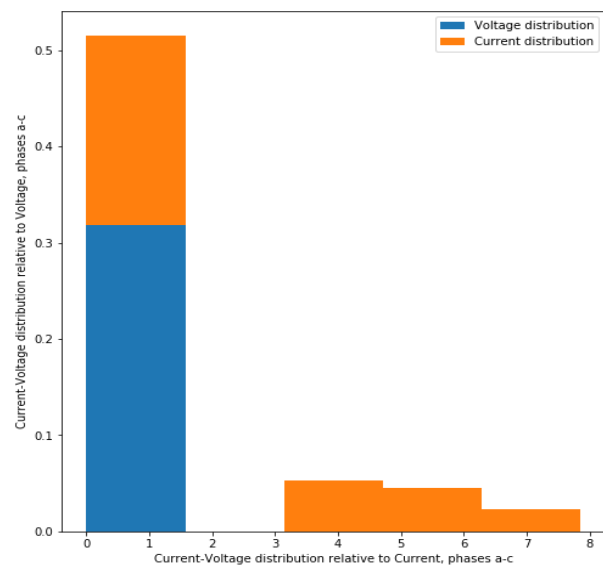


Fig. 11 Bivariate plot showing voltage and current distribution.

The Figs. 12- 14 show voltage for each type of fault, it shows the population of power system parameters for each type of fault. This helps to draw insight on what happens to the phase voltage values during each type of fault and this helps when making decisions during power system design and reliability studies.

Fig. 12 shows the distribution of voltages values across each fault type for phase 'a' during different fault conditions. During fault conditions associated with phase 'a', there is a decline in voltage values, whereas the voltage values for the fault types that are not associated with phase 'a' are observed to be intact.

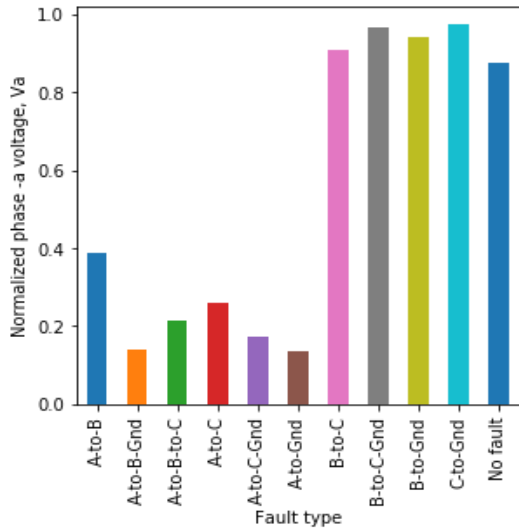


Fig. 12 Voltage distribution for phase 'a' for each fault type.

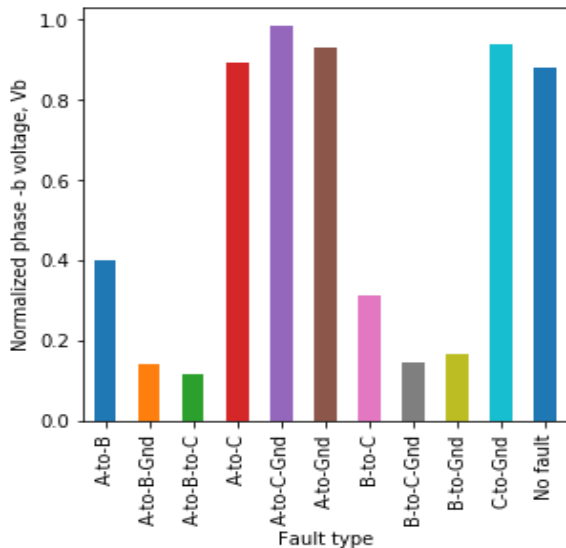


Fig. 13 Voltage distribution for phase 'b' for each fault type.

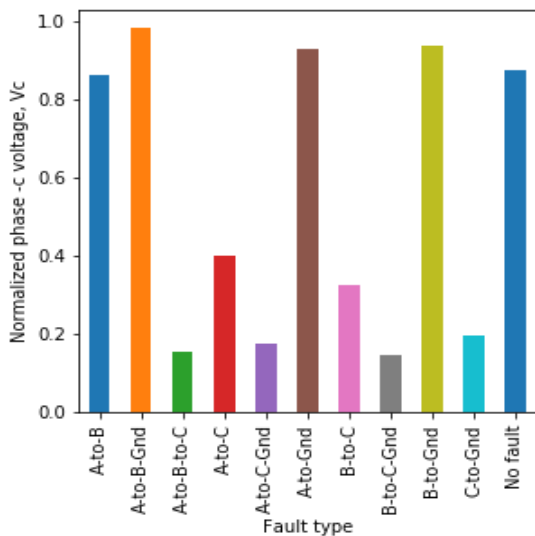


Fig. 14 Voltage distribution for phase 'c' for each fault type.

Similarly, Fig. 13 shows the distribution of voltages values across each fault type for phase 'b' during different fault conditions. During fault conditions associated with phase 'b' there is a decline in voltage values, whereas the voltage values for the fault types that are not associated with phase 'b' are intact. In addition, Fig. 14 the distribution of voltages values across each fault type for phase 'c' during different fault conditions. Observation of Fig. 14 shows that during fault conditions associated with phase-a there is a decline in voltage values, whereas the voltage values for the fault types that are not associated with phase 'c' are intact.

The electric current distribution can be shown in like manner as seen shown in Figs. 15 to 17 for a different type of fault, and current values during each type of fault help when making decisions during power system design and reliability studies.

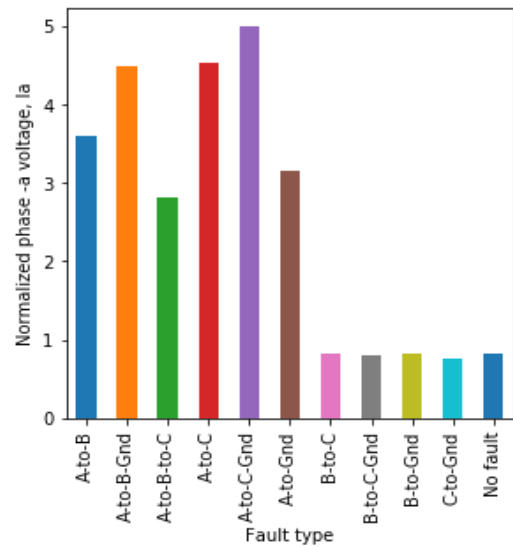


Fig. 15 Current distribution for phase 'a' for each fault type.

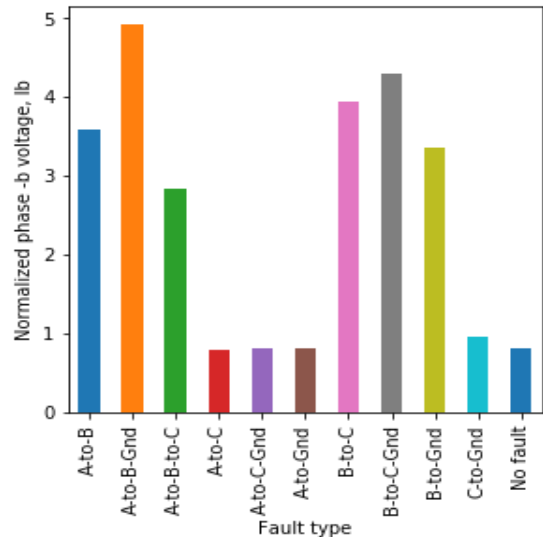


Fig. 16 Current distribution for phase 'b' for each fault type.

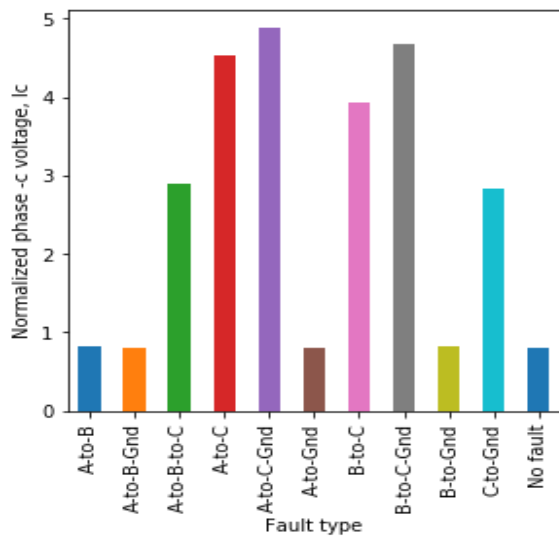


Fig. 17 Current distribution for phase 'c' for each fault type.

Fig. 15 depicts the distribution of current values across each fault type for phase 'a', in contrast to what was obtained in the distribution from the bar-graphs for the voltage values during fault conditions associated with phase 'a', there is a rapid rise in current values whereas the current values for faults not associated with phase 'a' remained unchanged. Also, Fig. 16 shows the distribution of current values across each fault type for phase 'b'. Observation shows that during fault conditions associated with phase 'b' there is a rapid rise in current values whereas the current values for faults not associated with phase 'b' remained unchanged. Besides, Fig. 17 depicts the distribution of current values across each fault type for phase 'c'. It was observed that during fault conditions associated with phase 'c' there is a rapid rise in current values whereas the current values for faults not associated with phase 'c' remained unchanged.

3.3. Model Validation

Validation is necessary when building a neural network model and it is usually represented by a validation curve. A validation curve, shown in Fig. 18, gives a measure of how effective an estimator fares with data with which it has been trained and also measures how well it handles new or unrecognizable inputs. Having split the data sets into the training set and test set; the validation curve shows how well the model was able to handle new datasets (the test set) after being trained with the (train set).

The accuracy of the model is basically a measure of a ratio of the amount of data

correctly predicted to the total amount of data passed into the model, sequel to obtaining the model accuracy. It is important to observe how easily the model made the predictions and this is evaluated by plotting a confusion matrix. As the name implies, it essentially provides an insight on how well the model was able to predict the outcome of the test dataset and also issues encountered in making the prediction. The confusion matrix, shown in Fig. 19, showed that the model was considerably decisive in classifying each type of fault with minimal confusion. This suggests that the model was well trained and has a good grasp of the patterns associated with each fault and can easily classify other datasets when the need arises.

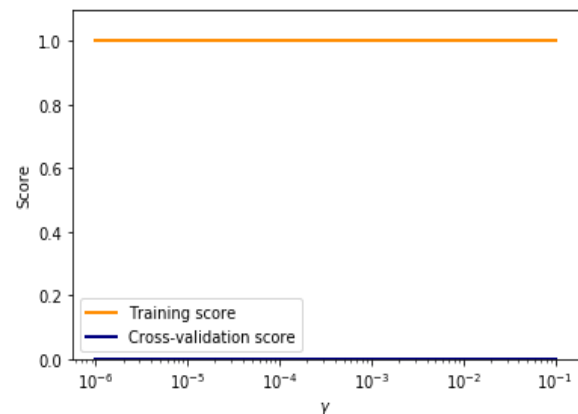


Fig. 18 Validation plot for the model.

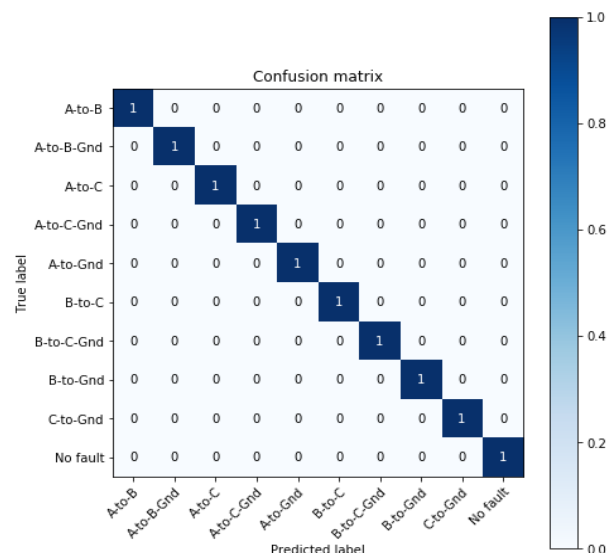


Fig. 19 Confusion matrix for the tested data.

Artificial neural network is a very handy tool for fault analysis and detection. Neural networks built on complex statistical methods and optimization techniques and as such, they are generally complex. The model developed in this paper describes how to effectively deploy a neural network using systematically

designed python programming libraries that simplify the scientific complexities presented by neural networks. The model produced a 90% training result and a 100% prediction accuracy.

This paper contributes to the existing string of research on faults analysis using ANN as an alternative method, which is characterized by simplicity, without sacrificing the accuracy of the method. One main limitation of the proposed approach is that it leverages on data availability to accurately classify and predict faults, which make it to be data-intensive. The approach presented in this paper identifies and classifies various unsymmetrical faults through the use of ANN. The approach presented in this paper could also be extended to predict symmetrical faults in distribution networks. Although, the approach is tested using a small distribution network of 11 kV distribution network of University of Lagos, it can be extended to larger sized practical power systems. One important factor that constrained this present study to a small network is the availability of datasets, which has a greater influence on the results obtained from the study.

4. Conclusion

In this paper, the application of an artificial neural network for classifying various unsymmetrical faults occurring on a typical 11 kV distribution network of the University of Lagos in Nigeria. The relevant mathematical formulations based on the suggested approach have been presented. The datasets obtained for the test case are sectioned into two parts; the first part is used to train the model while the validation and integrity of the developed model are tested using the second portion. The results obtained showed that the method is able to accurately locate and classify all types of unsymmetrical faults on the system. It is seen that proper data visualization and cleaning plays a significant role in the learning process, performance and accuracy of a neural network model. Moreover, based on the results obtained, it can be inferred that the approach presented could be helpful to system operator by optimizing the speed in classifying unsymmetrical faults, most especially, during critical outages, so as to reduce downtimes and avoid lengthy blackouts. Although a simple system is used for the validation of the approach in this present study, larger networks could also be tested as part of the future studies.

Conflict of Interests

The authors declare that there is no conflict of interests regarding the publication of this paper.

ORCID

Akintunde Alayande <https://orcid.org/0000-0003-1503-2171>

Olakunle Olabode <https://orcid.org/0000-0002-8163-2506>

Okwuchukwu Nwankwoh <https://orcid.org/0000-0003-1749-9007>

References

- [1] P. O. Akadiri, E. A. Chinyio, and P. O. Olomolaiye, "Design of a sustainable building: a conceptual framework for implementing sustainability in the building sector," *Buildings*, vol. 2, no. 2, pp. 126–152, 2012.
- [2] A. Akhikpemelo, M. J. E. Evbogbai, and M. S. Okundamiya, "Fault detection on a 132kV transmission line using artificial neural network," *Int. Review Electr. Eng.*, vol. 14, no. 3, pp. 220–225, 2019.
- [3] A. Elnozahy, K. Sayed, and M. Bahyeldin, "Artificial neural network-based fault classification and location for transmission lines," *IEEE Conference on Power Electronics and Renewable Energy*, Aswan city, Egypt, 23 - 25 October, 2019, pp. 140–144.
- [4] J. A. García-García, J. G. Enríquez, M. Ruiz, C. Arévalo, and A. Jiménez-Ramírez, "Software process simulation modeling: systematic literature review," *Comput. Stand. Inter.*, vol. 70, p. 103425, 2020, doi: 10.1016/j.csi.2020.103425
- [5] M. Ghasempour, J. Heathcote, J. Navaridas, L. A. Plana, J. Garside, and M. Luján, "Analysis of software and hardware-accelerated approaches to the simulation of unconventional interconnection networks," *Simul. Model. Pract. Th.*, vol. 103, p. 102088, 2020, doi: 10.1016/j.simpat.2020.102088.
- [6] H. Le-Huy and G. Sybille, "MATLAB/Simulink and PSPice as modeling tools for power systems and power electronics," *2000 Power Engineering Society Summer Meeting (Cat. No.00CH37134)*, Seattle, WA, 2000, pp. 766–767 vol. 2, doi: 10.1109/PESS.2000.867449
- [7] J. G. Ross, C. F. Franzke, and L. A. Schuh, "The spice 3 programming language and its application to power system analysis," *IEEE Trans. Power Syst.*, 1988, vol. 3, no. 4, pp. 1872–1876.
- [8] J.-H. Chen, "Industrial power system analysis with database access," *IEEE Trans. Ind.*, vol. 36, no. 5, pp. 1198–1205, 2000.
- [9] W. Xu, Y. Liu, D. Koval and M. A. Lipsett, "Using spreadsheet software as a platform for power system analysis," *IEEE Comput. Appl. Power*, vol. 12, no. 1, pp. 41–45, 1999.
- [10] T. Adu, "A new transmission line fault locating system," *IEEE Trans. Power Del.*, vol. 16, no.

- 4, pp. 498–503, 2001.
- [11] M. J. Reddy and D. K. Mohanta, "Adaptive-neuro-fuzzy inference system approach for transmission line fault classification and location incorporating effects of power swings," *IET Gener. Transm. Dis.*, vol. 2, no. 2, pp. 235–244, 2008.
- [12] N. A. Sundaravaradan et al., "Wavelet based transmission line fault analysis: a literature survey," *2014 14th Int. Conference on Environment and Electrical Engineering*, Krakow, 10 - 12 May, 2014, pp. 254-259.
- [13] A. Prasad, J. Belwin Edward, and K. Ravi, "A review on fault classification methodologies in power transmission systems: Part-I," *J. Electr. Syst. Inform. Technol.*, vol. 5, no. 1, pp. 48–60, 2018.
- [14] D. C. Robertson, O. I. Camps, J. S. Mayer, and W. B. Gish, "Wavelets and electromagnetic power system transients," *IEEE Trans. Power Del.*, vol. 11, no. 2, pp. 1050–1056, 1996.
- [15] H. Eristi, "Fault diagnosis system for series compensated transmission line based on wavelet transform and adaptive neuro-fuzzy inference system," *Measurement*, vol. 46, no. 1, pp. 393–401, 2013.
- [16] A. M. Stankovic and T. Aydin, "Analysis of asymmetrical faults in power systems using dynamic phasors," *2000 Power Engineering Society Summer Meeting (Cat. No.00CH37134)*, Seattle, WA, 2000, pp. 1957 vol. 3, doi: 10.1109/PESS.2000.868834
- [17] M. Oleskovicz, D. V. Coury, and R. K. Aggarwal, "A complete scheme for fault detection, classification and location in transmission lines using neural networks," in *7th Int. Conference on Developments in Power Systems Protection*, 2001, no. 479, pp. 335–338.
- [18] M. Sanaye-Pasand and H. Khorashadi-Zadeh, "Transmission line fault detection & phase selection using ANN," *Int. Conference on Power Systems Transients, New Orleans, USA*, vol. 2, no. 1, pp. 1–6, 2003.
- [19] O. Peter and A. Isaac, "An artificial neural network-based intelligent fault classification system for the 33-kV Nigeria transmission line," *Int. J Appl. Eng. Res.*, vol. 13, no. 2, pp. 1274–1285, 2018.
- [20] J. Jiao, M. Zhao, J. Lin, and K. Liang, "A comprehensive review on convolutional neural network in machine fault diagnosis," *Neurocomput.*, vol. 417, pp. 36–63, 2020.
- [21] O. E. Obi, "An extended ann-based high speed accurate transmission line fault location for double phase to earth fault on non-direct-ground," *Int. J Eng. Sci. Technol.*, vol. 1, no. 1, pp. 31–47, 2019.
- [22] V. C. Ogbob, and T. C. Madueme, "Investigation of faults on the Nigerian power system transmission line using artificial neural network," *Int. J Res. Manage. Sci. Technol.*, vol. 3, no. 4, pp. 87–95, 2015.
- [23] O. Peter, S. Oluwaseun, and A. Ayokunle, "Fault identification system for electric power transmission lines using artificial neural networks," *Int. J. Sci. Eng. Res.*, vol. 9, no. 2, pp. 678–685, 2018.
- [24] M. Jamil, S. K. Sharma, and R. Singh, "Fault detection and classification in electrical power transmission system using artificial neural network," *SpringerPlus*, vol. 4, p. 334, 2015, doi: 10.1186/s40064-015-1080-x.
- [25] K. Nagar and M. Shah, "A review on different ann based fault detection techniques for HVDC systems," *Int. J Innov. Res. Eng. Manage.*, vol. 3, no. 6, pp. 477–481, 2016.
- [26] W. Chen and K. Shi, "A deep learning framework for time series classification using relative position matrix and convolutional neural network," *Neurocomput.*, vol. 359, pp. 384–394, 2019.
- [27] M. Gridach, "A framework based on (probabilistic) soft logic and neural network for NLP," *Appl. Soft Comput.*, vol. 93, p. 106232, 2020, doi: 10.1016/j.asoc.2020.106232
- [28] S. Armoogum and X. Li, "Big data analytics and deep learning in bioinformatics with hadoop", in *Deep Learning and Parallel Computing Environment for Bioengineering Systems*, A. K. Sangaiah, Ed. Academic Press, 2019, pp. 17–36.
- [29] H. Jiang, Z. Xi, A. A. Rahman, and X. Zhang, "Prediction of output power with artificial neural network using extended datasets for Stirling engines," *Appl. Energy*, vol. 271, p. 115123, 2020, doi: 10.1016/j.apenergy.2020.115123
- [30] T. B. Lopez-Garcia, A. Coronado-Mendoza, and J. A. Domínguez-Navarro, "Artificial neural networks in microgrids: a review," *Eng. Appl. Artif. Intell.*, vol. 95, p. 103894, 2020, doi: 10.1016/j.engappai.2020.103894
- [31] B. Li, Y. Lee, W. Yao, Y. Lu, and X. Fan, "Development and application of ann model for property prediction of supercritical kerosene," *Comp. Fluids*, vol. 209, p. 104665, 2020, doi: 10.1016/j.compfluid.2020.104665
- [32] S. Vasantharathna, "Electric power systems," in *Electric Renewable Energy Systems*, M. H. Rashid, Ed. Boston: Academic Press, 2015, pp. 403–456.